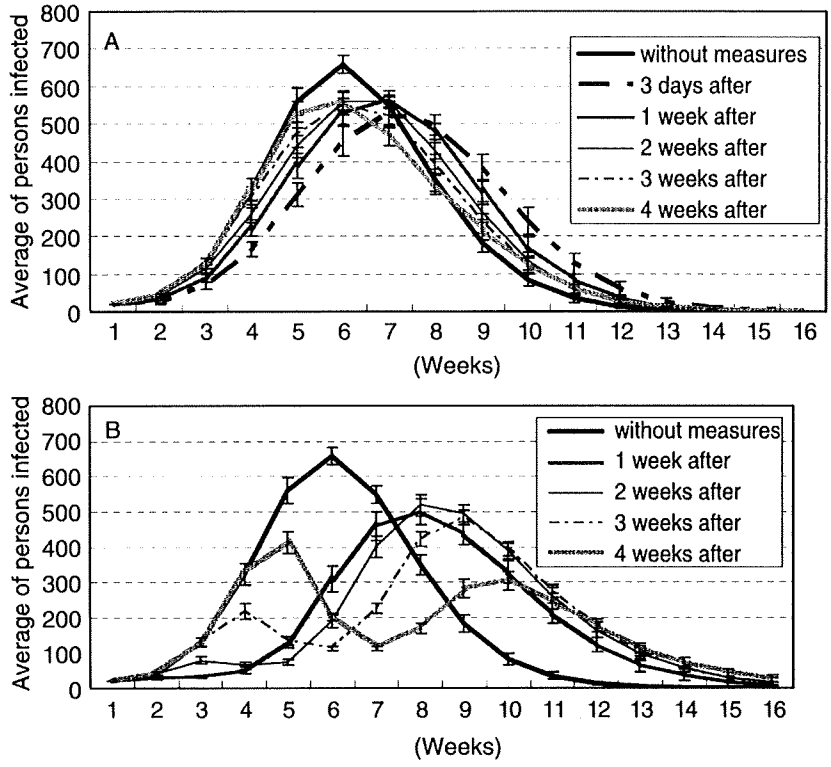

FIGURE 5. Delay and peak shift of newly infected with PT and SC. **A** The average of 100 cases of persons infected with traffic prohibition (1) 3 days, (2) 1 week, (3) 2 weeks, (4) 3 weeks and (v) 4 weeks after the beginning of the epidemic. **B** The average of 100 cases of persons infected if schools were closed for (1) 1, (2) 2, (3) 3, and (4) 4 weeks after the beginning of the epidemic. *Bars* indicate 95% confidence interval.

ison of the effect of the time lag to the closing of schools, SC starting (1) 1, (2) 2, (3) 3, and (4) 4 weeks after the beginning of the epidemic is compared in Figure 5B. The average of the total number of newly infected was 2,756 for (1), 2,895 for (2), 2,820 for (3), and 2,696 for (4). Although there is a noticeable difference in the shapes of the lines in Figure 5B, the variation of the total number of infected in the cases of SC is less than 9% of infected people in the case without any implemented preventative measures.

In Table 2, we show the total number of persons infected, the day of the peak of infection, and the sum of the average numbers of infected before the peak in the case of PT or SC. PT and SC changed only the location of the infected people. The variation of the total number of infected is not large, but both measures delay the peak of the epidemic. PT within 2 weeks after the beginning of the epidemic delayed the peak by 1 week compared to the case without any implemented preventative measures. SC within 3 weeks delayed the peak of the epidemic more than 2 weeks.

We combined PT, SC, and VSC. Figure 6A shows the results of multiple measures. In this case, 2-week PT and 2-week SC started with the fourth week after the beginning of the epidemic. With VSC, 30% of children became unsusceptible.

TABLE 2. Delay and peak shift of newly infected with the implementation of PT and SC

		First peak		Second peak	
Measure	Total number	Week	Sum of infected	Week	Sum of infected
None	2,951	6	1,734	–	–
PT					
3 days	2,909	7	1,567	–	–
1 week	2,943	7	1,884	–	–
2 weeks	2,915	7	1,994	–	–
3 weeks	2,874	6	1,511	–	–
4 weeks	2,837	6	1,598	–	–
SC					
1 week	2,756	8	1,528	–	–
2 weeks	2,895	3	140	8	1,390
3 weeks	2,820	4	408	9	1,784
4 weeks	2,696	5	928	10	1,995

PT Prohibition of traffic, *SC* school closure.

The total number of infected is 2,539 with SC and PT, 1,578 with SC and VSC, 1,643 with PT and VSC, and 955 with all three measures. Figure 6B shows the results of VSC in combination with 2-week PT starting with the fourth week after the beginning of the epidemic. Figure 6C shows the results of VSC in combination with 2-week SC starting with the fourth week after the beginning of the epidemic. For VSC, unsusceptible children are assumed to be 5%, 10%, 20%, and 30%.

DISCUSSION

Characteristics of the Spread of a Seasonal Epidemic of Influenza along the Chuo Line in Tokyo and Validity of the Simulation

In our simulation, we analyzed places where people would become infected. When the infection began to spread, people were infected mainly in trains, but this number remained small. Many people then became infected in schools and at home, demonstrating that the spread of influenza along the Chuo Line occurs in two periods, the first beginning 2 weeks after the beginning of epidemic, followed by the second period. During the first period, commuters were infected in trains and then introduced influenza into their towns, and some children were infected at home. During the second period, many children were infected in schools and then in turn infected their parents at home. The number of persons infected increased exponentially during the second period.

In our analysis, profiles of real influenza data in Tokyo for four winter seasons are similar, except in late winter of 2004–2005. This suggests there is a stable mechanism of transmission of influenza along the Chuo Line. The profiles of the simulation are also similar to those of the real data, especially considering that the peaks 6 weeks after the beginning of the epidemic in the simulation almost coincided with that of the real data measured from the beginning of the outbreak. This indicates that the model for the simulation of the spread of influenza reflected the mechanism of the real spread of influenza.

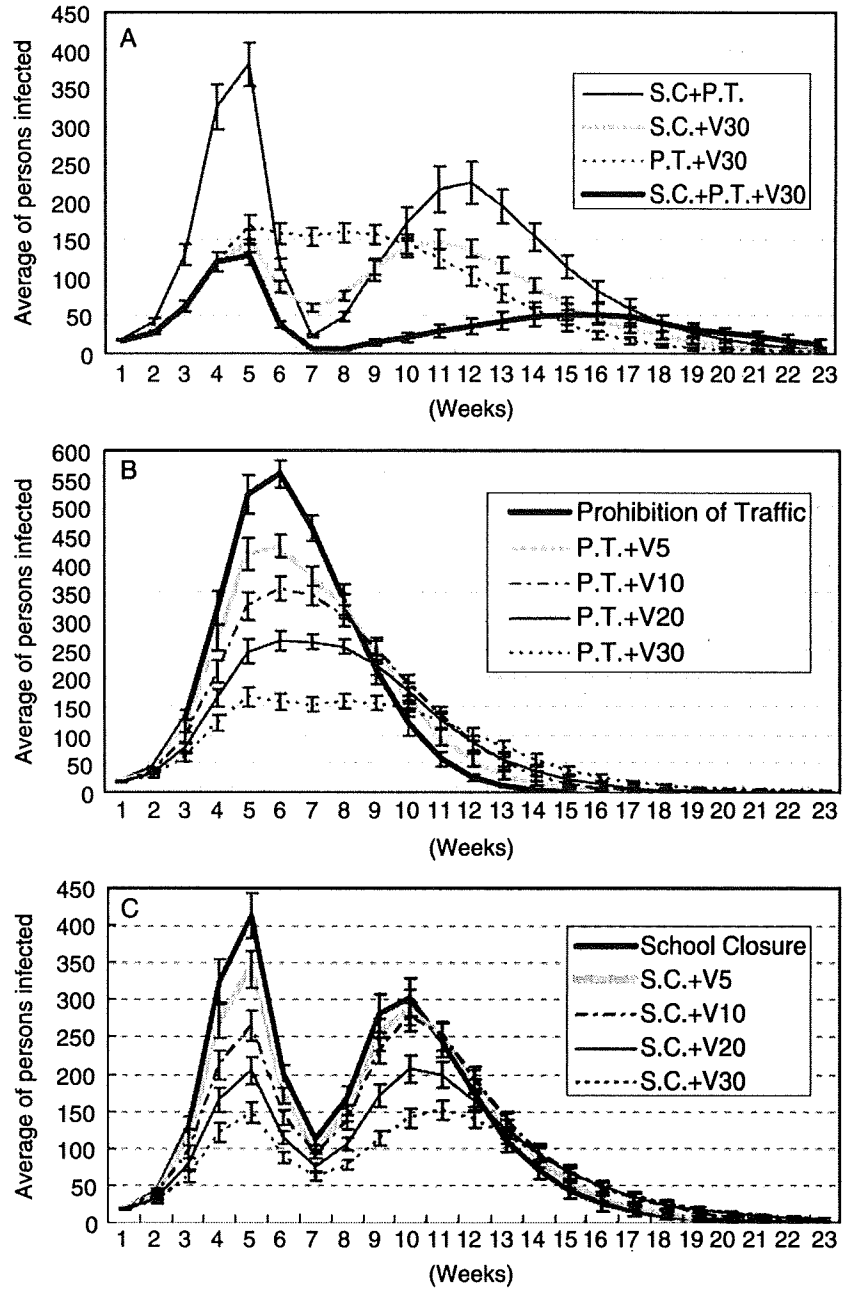

FIGURE 6. Effects of combination of measures, including 2 week PT and 2 week SC beginning in the fourth week, on an average of 100 cases of persons infected. V5-30: vaccination of school children where 5–30% of school children, respectively, become unsusceptible.

On the other hand, the real data of the NIID database provided evidence of the effectiveness of social distancing for protection against influenza. There is a small peak in some of the real data profiles at the beginning of the spread of influenza. The weeks when the peaks declined coincided with the New Year holidays. In Japan, schools are

closed for 2 weeks at this time, and almost all businesses are closed for 1 week; many people in Tokyo return to their home provinces. We conjecture that changes in human behavior during the New Year holidays caused these small peaks.

PT

Influenza was transmitted into commuter towns along the Chuo Line by commuters. However, it would be difficult to prohibit traffic while the number of infected was small; thus in the present study, we prohibited traffic after the pre-epidemic spread of influenza. The profile of the number of infected persons by PT was similar to that without prohibition, and the decrease of the number of infected persons by PT was small. This shows that PT is not effective for protection after the introduction of the spread of influenza into the suburbs. Similarly, Germann et al.[11] demonstrated in their simulation that the number of ill people did not decrease, even though they reduced long-distance travel in the United States to 10% of normal frequency.

We surmised that PT would be effective because influenza is believed to be transmitted in trains used by approximately one tenth of suburban commuters. However, our simulation disproved this supposition. After influenza was transmitted to the suburbs, the number of persons infected in schools and homes was larger than the number of persons infected in trains. Because of the nature of human contact in train compartments, the number of persons infected increased exponentially with the passage of time. Commuters spend 1–2 h in trains, and children spend 6 h or more at school. Thus, children play a more crucial role in spreading influenza than commuters after the influenza is introduced into towns.

These results suggest that towns would be protected from the spread of disease if we could prohibit traffic before the introduction of the epidemic. However, complete protection is difficult because commuters may be already infected before the detection of the spread of influenza. Our results show the spread of the epidemic occurs in the towns even if traffic is prohibited for 3 days after the beginning of the epidemic. However, early PT delays the spread of disease. The increase in the number of infected in cases of 3 days, 1 week, and 2 weeks was smaller than the case without any preventative measures implemented. This indicates that introduction of the epidemic into towns by infected commuters decreased in the early stages in our simulation.

In our simulation, the spread of influenza was initially introduced into local commuter towns by commuters. A similar role of transmission by travelers is discussed using real data. Hollingsworth et al.[23] reported that frequent travelers accelerate the international spread of the epidemic of respiratory disease only if they are infected early in an outbreak, and the outbreak does not expand rapidly. Brownstein et al.[24] demonstrated air travel may be an important mode of long-range dissemination of influenza in the United States. Moreover, Viboud et al.[25] also showed the strong dependence of inter-pandemic influenza spread on workflow implies a key role for adults in the regional dissemination of influenza; at the same time, the long-distance dissemination of influenza between cities or states is captured by movements linked to adults.

SC

In the present study, we closed schools for 2 weeks from the fourth week after the beginning of the epidemic because school was not closed until a certain number of children became infected, and in Japan, the period of SC is usually 1 or 2 weeks. In this case, the peak of the number of children infected was lowered, but the period of the epidemic was prolonged. When we reopened the schools, the number of infected again

increased. While the schools were closed, many infected children recovered. Because children who recovered divided a long linkage of transmission into shorter linkages, the increase of the number of persons infected is slower than before SC, but the decrease of the total number of persons newly infected was small. The results show that SC delays the transmission but somewhat decreases the scale of the epidemic. We achieved the same results in SC in an isolated town, reported elsewhere.[14]

SC 4 weeks after the beginning of epidemic, a conventional measure, is effective in decreasing the peak of infection. A prominent peak appeared in the early stage, but it did not appear in the cases of SC before 2 weeks, and the ripple is small in the case of 3 weeks. This simulation suggests that SC before 3 weeks from the beginning of the epidemic may delay the spread more than 2 weeks.

The characteristics of SC have been studied mainly by simulation. Although their model was designed for enteric virus, Elveback et al.[2] study the effect of opening or closing grade schools. They demonstrate that schools provide additional pathways for the spread of disease between families and between family clusters (neighborhoods or other social groups). Elveback et al.[3] asserted closing school for a few days after an influenza epidemic has begun is more effective in mitigating the duration than the size of the disease. In Asian flu infection in the winter seasons of 1957–1958, Glass et al.[26] reported that closing schools and keeping children and teenagers at home reduced the infection rate by less than 90%. Glass and Barnes[27] showed that closing schools can considerably reduce transmission among children but has only a moderate impact on average transmission rates among all individuals (both adults and children). Also, Ferguson et al.[28] showed SC during the peak of a pandemic can reduce peak infection rates by up to 40% but with little impact on overall infection rates.

The decrease of the number of persons infected by SC for 2 weeks in the simulation seems similar to the real data during the New Year holidays. We can regard the similarity between the real data of surveillance and the simulation of SC as evidence of the effect of the behavior change of children. For real data, Heymann et al.[29] reported evaluation of the effect of SC on the occurrence of respiratory infection among children ages 6–12 years old with a significant decrease in health care services during the period of SC. Vynnycky and Edmunds[30] reported, using the data of Asian influenza, that a modest reduction, e.g., 22%, might be possible if schools were closed early and the basic reproduction number were low. Valleron and Flahault[31] also reported a delay of 10–20 days between school holidays and a decrease in the incidence of influenza diagnoses from 1984 to 2000 in France. The real data show a significant relation between SC and spread of influenza. Based on the simulations, we assert that early SC produces a delay of the spread of influenza and effectively reduces the peak, but that we cannot expect a significant decrease of the total number of persons infected.

VSC

We vaccinated children instead of adults because systematic vaccination of adults seemed difficult due to lifestyle differences. The results of our simulation show that the decrease of the number of persons infected was not proportional to the percentage of unsusceptible children. However, a distinctive trend in the simulation was that the number of persons infected at home decreased when the number of children infected in schools decreased. This strongly suggests that VSC may stop the spread of influenza not only in children, but also in adults because a proportion of vaccinated children who become immune may interrupt the linkage of transmission in the regional community. Although the number of children and adults infected in schools and at home decreased, the number of persons infected in trains did not decrease significantly concomitant

with the VSC. These results suggest that the course of infection primarily among adults in trains is independent of the course of infection in schools and at home.

Our simulation data strongly suggest that VSC is effective in preventing the spread of influenza in the regional community, notwithstanding the important role played by commuters in the initial phase. In Japan, children were mass-vaccinated by law from 1962 to 1987, but in 1987, the law was relaxed and then repealed in 1994. According to research on deaths from pneumonia and influenza from the 1950s to the 1990s, mortality of the elderly decreased when school children were vaccinated,[1] but the effectiveness of VSC is still under discussion.[15–17] The same subject has been studied in the United States.[18–21] These studies assert the effectiveness of school-based influenza vaccination. The Tecumseh case is well known for the effectiveness of vaccinated children in protecting a regional community.[22]

In the present simulation, we analyzed PT or SC, as, under the Japanese Vaccination Law, we cannot prepare for school-based mass vaccination before the influenza season. This study suggests the effectiveness of the combination of different measures. It takes almost 2 weeks for the effect of vaccination to appear. As children are not vaccinated before influenza season, the allowance of time before the spread of the epidemic among children is important for mass vaccination. Delay of spread by SC 2 or 3 weeks after the beginning of the epidemic presents the opportunity for mass vaccination. Our simulation may recommend children be vaccinated before the spread in schools, when we can detect the epidemic in its early stages in trains and then soon close the schools. The effect of mass VSC is expected to decrease the total number of infected in the communities. Ferguson et al.[28] reported that a staged vaccination program has the maximum effect of reducing transmission if children are vaccinated first because school-aged children have the highest transmission rate, while vaccinating the elderly first has the lowest impact on transmission. Germann et al.[11] studied 'dynamic vaccination', in which the vaccine became available incrementally, and showed that the number of ill persons of dynamic child-first vaccination is less than that of dynamic vaccination.

Our results show that VSC has the effect of protecting communities, even if the vaccine is low-efficiency. The problem of low-efficiency vaccine is important, especially when there is a small stockpile of vaccine. Riley et al.[32] reported that substantial reductions in the infection rate are likely to happen and also increase individual-level protection, if vaccines are given to more people at a lower dose. The population-level implications of pre-pandemic vaccine programs should be considered when deciding on stockpile size and dose. Germann et al.[11] compared the recommended two doses, assumed to confer the best protection level, with a strategy in which twice as many people are given a single dose; this assumes that a single dose confers about half the protection of two doses, and that the number of ill persons in the one-dose regimen is less than in the two-dose regimen. Wu et al.[33] reported the problem of the spatial allocation of pre-pandemic influenza vaccination related to the low efficiency of the vaccine.

Multiple Measures

The synergistic effect depends on the combination of measures, i.e., when multiple measures are implemented. When we close schools and prohibit traffic at the same time, the decrease of persons infected in the seventh week is greater than when we combine either SC and VSC or PT and VSC. This is because in our simulation, during an epidemic, people stay home all day and come in contact only with their families.

However, the synergistic effect of combining measures may not always be positive. When combining SC and VSC, the effect of VSC diminished when schools were closed. VSC and SC reduced the spread of influenza in the community by

protecting children. Because there is a similarity in the effect of both measures, a synergistic effect could not be expected. Germann et al.[11] reported that the estimated benefits of preferentially vaccinating children are offset by closing schools. Glass and Barnes[27] reported that immunization of all school children provides only a slight improvement over closing schools, indicating that schools are an important venue for transmission among children. In the combination of PT and VSC in our study, PT did not affect the efficiency of the vaccination. This indicates that the course of infection in trains is independent of the course of infection among children.

Our simulation strongly suggests the following:

1. There are two periods in the spread of influenza in the suburbs of Tokyo. The first period is defined as 2 weeks from the beginning of the epidemic; this is followed by the second period. In the first period, commuters introduce influenza into the suburbs, and in the second, children play an important role in the spread of influenza in the suburbs.
2. PT is not effective after the introduction of influenza into the suburbs. However, the epidemic would be delayed by $\approx$1 week in the early stage of the epidemic if traffic were prohibited within 2 weeks after the beginning of the epidemic.
3. SC would delay the epidemic and reduce peaks of infection. If we could close schools before 3 weeks after the beginning of the epidemic, the epidemic would be delayed by more than 2 weeks.
4. VSC is effective in preventing the spread of influenza, even when commuters spread the disease along a suburban railroad.
5. The synergistic effect of multiple measures depends on a combination of measures; SC offsets the effect of VSC in communities during the period of SC.

ACKNOWLEDGEMENTS

We thank Dr. Nobuhiko Okabe and the staff of the Infectious Disease Surveillance Center, NIID, for the preparation of the database of infection in Japan. We also thank Dr. Shigeyuki Itamura, Department of Virology III, and Dr. Hiroshi Yoshikura, former director of NIID, for suggesting the simulated study and for valuable discussions. This study was partly supported by a grant from the Japan Science and Technology Agency; the Ministry of Health, Labour and Welfare; and the Ministry of Education, Culture, Sports, Science and Technology.

REFERENCES

1. Reichert TA, Sugaya N, Fedson DS, Glezen WP, Simonsen L, Tashiro M. The Japanese experience with vaccinating children against influenza. *N Engl J Med.* 2001;344(12):889–896.
2. Elveback L, Ackerman E, Gatewood L, Fox JP. Stochastic two-agent epidemic simulation models for a community of families. *Am J Epidemiol.* 1971;93(4):267–280.
3. Elveback LR, Fox JP, Ackerman E, Langworthy A, Boyd M, Gatewood L. An influenza simulation model for immunization studies. *Am J Epidemiol.* 1976;103(2):152–165.
4. Longini IM, Seaholm SS, Ackerman E, Koopman JS, Monto AS. Simulation studies of influenza: assessment of parameter estimation and sensitivity. *Int J Epidemiol.* 1984;13 (4):496–501.
5. Seaholm SS, Ackerman E, Wu SC. Latin hypercube sampling and the sensitivity analysis of a Monte Carlo epidemic model. *Int J Biomed Comput.* 1988;23(1–2):97–112.

6. Longini IM, Koopman JS, Haber M, Cotsonis GA. Statistical inference for infectious disease. *Am J Epidemiol.* 1988;128(4):845–859.
7. Addy CL, Longini IM, Haber M. A generalized stochastic model for the analysis of infectious disease final size data. *Biometrics.* 1991;47(3):961–974.
8. Longini IM, Halloran ME, Nizam A, Yang Y. Containing pandemic influenza with antiviral agents. *Am J Epidemiol.* 2004;159(7):623–633.
9. Longini IM, Nizam A, Xu S, et al. Containing pandemic influenza at the source. *Science.* 2005;309(5737):1083–1087.
10. Ferguson NM, Cummings DAT, Cauchemez S, et al. Strategies for containing an emerging influenza pandemic in Southeast Asia. *Nature.* 2005;437(7056):209–214.
11. Germann TC, Kadau K, Longini IM, Macken CA. Mitigation strategies for pandemic influenza in the United States. *Proc Natl Acad Sci USA.* 2006;103(15):5935–5940.
12. Arino J, van den Driessche P. A multi-city epidemic model. *Mathematical Population Studies.* 2003;10(3):175–193.
13. The NHK Broadcasting Culture Research Institute. *National Time Use Survey 2000 Report.* Tokyo: Japan Broadcast Publishing; 2001.
14. Yasuda H, Yoshizawa N, Suzuki K. Modeling on social spread from immunity. *Jpn J Infect Dis.* 2005;58(6):S14–15.
15. Hirota Y, Kaji M. Scepticism about influenza vaccine efficiency in Japan. *Lancet.* 1994;344(8919):408–409.
16. Hirota Y, Fedson DS, Kaji M. Japan lagging in influenza jabs. *Nature.* 1996;380 (6569):18.
17. Inoue S, Kramer MH, Fukuda K, et al. Vaccination of Japanese schoolchildren against influenza. *N Engl J Med.* 2001;344(25):1946–1948.
18. White T, Lavoie SL, Nettleman MD. Potential cost saving attributable to influenza vaccination of school-aged children. *Pediatrics.* 1999;103(6):e73.
19. Longini IM, Halloran ME. Strategies for distribution of influenza vaccine to high-risk groups and children. *Am J Epidemiol.* 2005;161(4):303–306.
20. King JC, Stoddard JJ, Gaglani MJ, et al. Effectiveness of school-based influenza vaccination. *N Engl J Med.* 2006;355(24):2523–2532.
21. Lucee BR, Zangwill KM, Palmer CS, et al. Cost-effectiveness analysis of an intranasal influenza vaccine for prevention of influenza in healthy children. *Pediatrics.* 2006;108(2): e24.
22. Monto AS, Koopman JS, Longini IM. Tecumseh study of illness. XIII. Influenza and disease, 1976–1981. *Am J Epidemiol.* 1985;121(6):811–822.
23. Hollingsworth TD, Ferguson NM, Anderson RM. Frequent travelers and rate of spread of epidemics. *Emerg Infect Dis.* 2007;13(9):1288–1294.
24. Brwonstein JS, Wolfe CJ, Mandl KD. Empirical evidence for the effect of airline travel on inter-regional influenza spread in the United States. *PLoS Med.* 2006;3(10):1826–1835.
25. Viboud C, Bjornstad ON, Smith DL, Simonsen L, Miller MA, Grenfell BT. Synchrony, waves, and spatial hierarchies in the spread of influenza. *Science.* 2006;312:447–451.
26. Glass RJ, Glass LM, Beyeler WE, Min HJ. Targeted social distancing design for pandemic influenza. *Emerg Infect Dis.* 2006;12(11):1671–1681.
27. Glass K, Barnes B. How much would closing schools reduce transmission during an influenza pandemic? *Epidemiology.* 2007;18(5):623–628.
28. Ferguson NM, Cummings DA, Fraser C, Cajka JC, Cooley PC, Burke DS. Strategies for mitigating an influenza pandemic. *Nature.* 2006;442(7101):448–452.
29. Heymann A, Chodick G, Reichman B, Kokia E, Laufer J. Influence of school closure on the incidence of viral respiratory diseases among children and health care utilization. *Pediatr Infect Dis.* 2004;23(7):675–677.
30. Vynnycky E, Edmunds WJ. Analyses of the 1957 (Asian) influenza pandemic in the United Kingdom and the impact of school closures. *Epidemiol Infect.* 2007;20:1–14 17445311, Apr.

31. World Health Organization Writing Group. Nonpharmaceutical interventions for pandemic influenza, national and community measures. *Emerg Infect Dis.* 2006;12 (1):88–94.
32. Riley S, Wu JT, Leung GM. Optimizing the dose of pre-pandemic influenza vaccines to reduce the infection attack rate. *PLoS Med.* 2007;4(6):1032–1040.
33. Wu JT, Riley S, Leung GM. Spatial considerations for the allocation of pre-pandemic influenza vaccination in the United States. *Proc Biol Sci.* 2007;274(1627):2811–2817.

Nephrol Dial Transplant (2007) 22: 77–87
doi:10.1093/ndt/gfl555
Advance Access publication 27 September 2006

Original Article

NDT
Nephrology Dialysis Transplantation

Up-regulation of adhesion molecule expression in glomerular endothelial cells by anti-myeloperoxidase antibody

Tomokazu Nagao[1], Mimiko Matsumura[1,2], Ayako Mabuchi[3], Akiko Ishida-Okawara[1], Osamu Koshio[4], Toshinori Nakayama[5], Haruyuki Minamitani[2] and Kazuo Suzuki[1]

[1]Department of Bioactive Molecules, National Institute of Infectious Diseases, Tokyo, Japan, [2]Graduate School of Science and Technology, Keio University, Yokohama, Japan, [3]Department of Physiology, University of Otago, Dunedin, New Zealand, [4]Department of Medicine, Teikyo University, Tokyo, Japan and [5]Graduate School of Medicine, Chiba University, Chiba, Japan.

Abstract

Background. Anti-neutrophil cytoplasmic antibody directed against myeloperoxidase (MPO-ANCA) has been implicated in pauci-immune crescentic glomerulonephritis. It stimulates primed neutrophils to adhere to glomerular endothelial cells (GECs), thereby releasing reactive oxygen and other toxic substances and ultimately damaging the GECs. Though, a pathogenic role for MPO-ANCA is not fully understood, we hypothesized that MPO-ANCA modulates GEC functions by the increases in expression of adhesion molecules.

Methods. A polyclonal rabbit anti-recombinant mouse MPO antibody (anti-rmMPO IgG) was evaluated in mouse GEC (mGEC) for its effect on adhesion molecule expression. The primary culture of mGEC was incubated with anti-rmMPO IgG or isotype control and the expression of intercellular adhesion molecules-1 (ICAM-1) was evaluated by real-time reverse transcription–polymerase chain reaction (RT–PCR) analysis and ICAM-1 cell ELISA.

Results. The real-time RT–PCR analysis showed that a treatment with 100 μg/ml anti-rmMPO IgG increased the expression of mRNAs for ICAM-1, vascular cell adhesion molecule-1 and E-selectin by approximately 12.5, 7.5 and 10.5-fold, respectively. ICAM-1 cell ELISA also substantiated increased expression of ICAM-1. This enhancement of ICAM-1 expression was mediated by the antigen specificity of anti-rmMPO IgG. In addition, there were several proteins in mGEC specifically immunoprecipitated with anti-rmMPO IgG.

Conclusions. These results showed that anti-MPO antibody activates not only neutrophils, but also GEC, indicating that anti-rmMPO IgG-induced direct activation of GEC contributes to neutrophil adhesion to GEC, thereby increasing glomerular neutrophil infiltration in initiation and progression of pauci-immune glomerulonephritis.

Keywords: adhesion molecules; crescentic glomerulonephritis; glomerular endothelial cells; MPO-ANCA

Introduction

Anti-neutrophil cytoplasmic antibody directed against myeloperoxidase (MPO-ANCA) are involved in the development of small vessel vasculitis such as idiopathic crescentic glomerulonephritis and microscopic polyangiitis [1–3]. MPO-ANCA has been used as a specific marker for these vasculitides, as evident from clinical observations that MPO-ANCA titres generally correlate with disease activity [4–6], although pathogenicity of the autoantibodies has not been clearly understood. Neutrophils have been reported to be a primary target of MPO-ANCA due to localization of MPO in the azurophilic granules of neutrophils and their translocation to plasma membrane upon priming with cytokines such as tumour necrosis factor-α (TNF-α) [7,8]. Therefore, previous studies have mainly focused on the signalling pathway in respiratory burst and degranulation of neutrophils stimulated with MPO-ANCA and initiation mechanisms of small vessel vasculitis by MPO-ANCA through neutrophil activation [9–12].

Adhesion of neutrophils to endothelial cells is an important step for neutrophil infiltration into glomeruli which is a histological feature of crescentic glomerulonephritis. Endothelial cells express cell surface counter receptors for integrins to be adhered with neutrophils in circulating blood and glomerular

Correspondence and offprint requests to: Kazuo Suzuki PhD, Chief of Biodefense Laboratory, National Institute of Infectious Diseases (NIID-NIH), Toyama 1-23-1, Shinjuku-ku, Tokyo 162-8640, Japan. Email: ksuzuki@nih.go.jp

endothelial cells express intercellular adhesion molecule-1 (ICAM-1) and vascular cell adhesion molecule-1 (VCAM-1). An elevated level of soluble ICAM-1 in sera of vasculitis patients has been reported [13–15]. Expression of the adhesion molecules on the surface of the endothelial cells is increased by stimulation with a wide variety of cytokines [16]. Similarly, elevated cytokine levels in the patient's blood seem to be a trigger for the enhancement of the expression of adhesion molecules on the surface, resulting in the development of vasculitis. However, a question remains whether ANCA also have direct effects on endothelial cells. Therefore, the direct effects of MPO-ANCA on the activation of glomerular endothelial cells must be elucidated in addition to the activation of neutrophils.

There are various studies available on the effects of sera or immunoglobulins from patients of autoimmune disease on endothelial cell activation. Johnson *et al.* [17] reported that autoantibody-positive serum samples from patients with vasculitis up-regulated ICAM-1 on human umbilical vein endothelial cells (HUVEC), although the molecular target of the autoantibody still remains unclear. De Bandt *et al.* [18] and Mayet *et al.* [19] demonstrated that anti-proteinase-3 antibodies from patients with Wegener's granulomatosis mediate ICAM-1 and VCAM-1 expression, respectively. Antibodies directed against endothelial cells from Scleroderma and Behçet's disease patients also activate HUVEC and up-regulated adhesion molecule expression [20,21]. However, the direct effect of MPO-ANCA on endothelial cells has not been investigated thus far. And, most research in this area has been done in HUVEC that can differ substantially from the cells in microvasculature, especially glomerular endothelial cells [22].

Here, we report the direct effect of polyclonal rabbit anti-recombinant mouse MPO antibody (anti-rmMPO) on expression of adhesion molecules in mouse glomerular endothelial cells (mGEC) and the mechanism of action.

Materials and methods

Primary culture of mouse glomerular endothelial cells and mesangial cells

We isolated mGEC from male C57BL/6 mice, which were maintained under specific pathogen-free conditions, according to the guidelines approved by the National Institute of Infectious Diseases Animal Care and Use Committee. Kidneys were obtained from freshly sacrificed mice perfused through the heart with cold Hank's balanced salt solution (HBSS) and glomeruli were prepared by a serial sieving method. Minced renal cortex tissue was serially passed through 150, 106 and 75 μm mesh stainless steel screens and glomeruli were collected using 53 μm mesh. The glomeruli, which contain small debris of renal tubule, were suspended in HBSS (Gibco-BRL Life Technologies, Gaithersburg, MD), washed twice by brief centrifugation (800 × *g*, 1 min) and digested in 1 mg/ml collagenase (Sigma, St Louis, MO) for 30 min at 37°C with occasional vortexing. Undigested glomeruli were pelleted by brief centrifugation and the supernatant containing single cell suspension of mGEC was suspended in growth medium [RPMI-1640 (Sigma) supplemented with 20% heat-inactivated foetal bovine serum (FBS, Gibco-BRL), 5 ng/ml vascular endothelial growth factor (VEGF) (Peprotech, Rocky Hill, NJ), 10 ng/ml bFGF (Sigma), 10 ng/ml epidermal growth factor (EGF) (Sigma), 20 U/ml heparin, 1 μg/ml hydrocortisone (Sigma), 50 U/ml penicillin and 50 μg/ml streptomycin (Gibco-BRL)] and plated on fibronectin-coated 35 mm dishes (Becton Dickinson, Franklin Lakes, NJ). Small colonies of mGEC were observed within 1 week after plating. To remove contaminating mesangial and epithelial cells, brief trypsinization was performed until a culture with purity over 90% of endothelial cells was achieved. The cells were maintained in collagen-coated 100 mm culture dish (Iwaki, Tokyo, Japan).

Mesangial cells were isolated from the outgrowth of the undigested glomeruli according to the method described by Deocharan *et al.* [23] and maintained in RPMI-1640 supplemented with 20% heat-inactivated FBS, insulin-transferrin-selenium supplement (Gibco-BRL), 50 U/ml penicillin and 50 μg/ml streptomycin.

Rabbit anti-recombinant mouse myeloperoxidase antibody

Anti-rmMPO antibody was prepared as described previously [24]. Briefly, rmMPO was prepared from *Escherichia coli* transfected with a plasmid containing MPO cDNA of mouse origin (C57BL/6). The expressed recombinant protein consisted of His-tag-L-chain-H-chain of mouse MPO. Anti-rmMPO IgG was raised by immunization of rabbit with purified rmMPO and IgG fraction of the polyclonal antibody was isolated from the serum using protein A (Amersham Biosciences Co., Piscataway, NJ). The reactivity to purified native mouse MPO was confirmed as shown previously [24]. Normal rabbit IgG was prepared by the same procedure except for non-immunization with rmMPO.

Antibody titre to rmMPO was measured as described previously [24]. Briefly, rmMPO was coated onto an ELISA plate (Toyoshima Co., Tokyo, Japan) overnight at 4°C. The plate was blocked with 1% bovine serum albumin (BSA) (Sigma) and then incubated with anti-rmMPO IgG for 1.5 h at room temperature. The bound anti-rmMPO IgG was detected by 2 h incubation with alkaline phosphatase-labelled anti-rabbit IgG antibody (Bio-Rad, Hercules, CA). The bound secondary antibodies were subsequently quantified by changes in the absorbance at 405 nm after incubation with 1 mg/ml p-nitrophenyl phosphate (Sigma).

Modification of antibody

To deplete IgG from the anti-rmMPO antibody, 1 ml of anti-rmMPO IgG varying the concentration from 0 to 200 μg/ml was incubated with or without protein A Sepharose [100 μl slurry in phosphate-buffered saline (PBS), Amersham Biosciences Co.] for 1 h at 4°C. The resultant supernatants after centrifugation (3000 × *g*, 5 min) were used for experiments. To adsorb MPO-specific antibody, we have taken advantage of the insolubility of the rmMPO in the absence of a high concentration of urea and used it to remove specific binding antibodies from anti-rmMPO IgG by adsorption [25].

Aggregated rmMPO was prepared by mixing and incubation with PBS for 1 h at 4°C. The aggregates were intensively washed with PBS until protein was undetectable in supernatant by UV absorption and incubated with 10 mg/ml anti-rmMPO IgG for 1 h at 4°C with agitation. As a control, the same amount of anti-rmMPO IgG was incubated in the absence of aggregated rmMPO. The mixture was centrifuged and supernatant was used for experiments. $F(ab')_2$ fragments were prepared using an ImmunoPure $F(ab')_2$ preparation kit (Pierce, Rockford, IL) according to the manufacturer's instructions.

Detection of ICAM-1 in mGEC (Cell ELISA)

The mGEC were plated on collagen-coated 96-well plates (Iwaki) at a density of 3×10^3 cells/well. At confluency, the cells were washed once with warmed HBSS and incubated for 1 h in RPMI-1640 medium containing 1% heat-inactivated FBS (assay medium). Anti-rmMPO IgG or control rabbit IgG diluted in assay medium was added to the wells and incubated for indicated periods, then the cells were washed with warmed PBS three times and fixed in 0.2% glutaraldehyde for 5 min at 4°C. For the blocking experiment, a neutralizing rat monoclonal antibody to TNF-α (BD Pharmingen, San Diego, CA) was included in assay medium throughout the incubation period. Non-specific binding was blocked by incubation with 1% BSA in PBS overnight at 4°C, followed by incubation for 1.5 h at room temperature with 0.5 μg/ml rat anti-mouse ICAM-1 monoclonal antibody (KAT-1; Chemicon, Temecula, CA). The primary antibody was detected by incubation for 1.5 h at room temperature with an alkaline phosphatase-conjugated anti-rat IgG antibody (1:2000, Bio-Rad). The bound secondary IgG was measured by the same procedure as aforementioned.

Detection of anti-endothelial cell antibodies

Anti-endothelial activity of antibodies used in this study was measured by the methods previously described by Carvalho *et al.* [20] with modification. mGEC were seeded onto a collagen-coated 96-well plates (Iwaki) at a density of 3×10^3 cells/well. The cells were fixed with 0.2% glutaraldehyde for 5 min at 4°C. The plates were blocked overnight with 1% BSA in PBS at 4°C and then incubated for 2 h with various concentrations of anti-rmMPO IgG or control IgG. The bound IgG was detected by an alkaline phosphatase-conjugated anti-rabbit IgG antibody (1:4000, Bio-Rad) with subsequent quantification of phosphatase using *p*-nitrophenyl phosphate as aforementioned. To measure the reactivity of anti-rmMPO IgG to live mGEC, the antibodies were first incubated with the live mGEC in the assay medium and then fixed with 0.2% glutaraldehyde. The bound IgG was measured by the same procedure as described before.

Immunoprecipitation

The anti-rmMPO or control rabbit IgG were bound to protein A Sepharose beads in lysis buffer [20 mM Tris–HCl, 150 mM NaCl, 1% NP-40, 0.5 mM phenylmethylsulphonyl fluoride (PMSF), pH 7.5] containing 0.1% BSA for 2 h at 4°C and washed several times with lysis buffer. Cells were lysed with lysis buffer and incubated with the antibody-bound protein A sepharose beads for 2 h at 4°C. The sepharose beads were washed three times with lysis buffer and bound proteins were solubilized by boiling in sodium dodecyl sulphate-polyacrylamide gel electrophoresis (SDS-PAGE) sample buffer. The protein samples were electrophoresed on 5–20% gradient gel and visualized by SYPRO Ruby staining (Molecular Probes, Eugene, OR).

Reverse transcript polymerase chain reaction (RT–PCR)

Total RNA was extracted using an ISOGEN (Nippongene, Tokyo, Japan), according to the manufacturer's instructions and quantified by UV absorption. One microgram of total RNA was reverse transcribed using ReverTra Ace-alpha (TOYOBO, Osaka, Japan). A semi-quantitative RT–PCR was used for the estimation of TNF-α mRNA expression. One microlitre of the resulting cDNA was used for PCR in 20 μl of Ex *Taq* buffer containing 0.2 mM dNTP mix, 0.5 μM of each primer and 25 U/ml Ex *Taq* polymerase (all reagents were purchased from TaKaRa Bio Inc.). Primer sequences for specific cDNA fragments were TNF-α: forward 5′-ctactgaacttcggggtgatcg-3′, reverse 5′-aagtctaagtacttgggca gattgac-3′, β-actin: forward 5′-atctggcaccacaccttctacaat gagctgcg-3′, reverse 5′-catcgtactcctgcttgctgatccacatctgc-3′. The amplification reactions were allowed to proceed for 30 cycles for TNF-α or 20 cycles for β-actin consisting of 94°C for 30 s, 55°C for 30 s and 72°C for 60 s. PCR products (10 μl) were electrophoresed on 2% agarose gels and stained with ethidium bromide. mRNA expression of ICAM-1, VCAM-1 and E-selectin was quantified by using a real-time RT–PCR. First-strand cDNA was synthesized as described above. One microlitre of cDNA samples was used for the PCR reaction and analysed by the ABI Prism 7000 Sequence Detection System (Applied Biosystems) using Taqman 2X Universal PCR Master Mix and Applied Biosystems Assays-on-Demand primers and Taqman probe sets specific for mouse ICAM-1, VCAM-1 and E-selectin, according to the manufacturer's instructions. A non-template control was included for each target analysed. Relative quantification of all targets was calculated by using the comparative cycle threshold method [26]. The levels of gene expression were standardized with those of the glyceraldehyde 3-phosphate dehydrogenase.

Immunofluorescence microscopy

Both mGEC and MC were plated on collagen-coated or non-coated glass coverslips (22 × 22 mm) in 35 mm culture dishes, respectively. The confluent monolayer was fixed in ice-cold methanol and blocked with 1% BSA in PBS overnight at 4°C. Rat monoclonal antibody to CD31 (MEC13.3, BD Pharmingen), or mouse monoclonal antibody to desmin (Sigma) diluted 1:100 in 1% BSA in PBS, were added onto each coverslip and the samples were incubated for 1 h at room temperature. The coverslips were washed three times with PBS and further incubated for 1 h at room temperature in FITC-conjugated goat anti-rat IgG antibody (Santa Cruz Biotechnology, Santa Cruz, CA) for CD31 or Alexa Fluor 488-conjugated anti-mouse IgG antibody (Molecular Probes) for desmin. The coverslips were washed and observed by

fluorescence microscopy. For the detection of ICAM-1, mGEC were incubated for 6 h with either 100 μg/ml anti-rmMPO or control IgG, fixed and immunostained for ICAM-1 using primary rat anti-mouse ICAM-1 monoclonal antibody and secondary FITC-conjugated goat anti-rat IgG antibody.

Statistical analysis

All data are expressed as mean ± SD. For individual comparisons, Student's *t*-test or Welch's corrected *t*-test, where appropriate, were used and differences with $P < 0.05$ were considered significant.

Results

Characterization of the primary mGEC

The population of the cells isolated from mice was characterized as endothelial cells by homogeneous monolayer of phase contrast image (Figure 1A) and positive staining with anti-CD31 (Figure 1B) in the junctional area and negative with anti-desmin (Figure 1C). The negative staining with anti-desmin indicates that there was little contamination of mesangial cells in the primary culture. In addition, RT–PCR analysis confirmed that mRNA of CD31 was expressed in the mGEC, but not in the mesangial cells (data not shown).

Up-regulation of adhesion molecule expression by anti-rmMPO IgG

To determine the direct effect of anti-rmMPO IgG on endothelial cell function, transcription levels of adhesion molecules in anti-rmMPO IgG-treated mGEC were examined. As shown in Figure 2A, quantitative RT–PCR revealed increases in mRNA levels of ICAM-1, VCAM-1 and E-selectin upon treatment with anti-rmMPO IgG in a dose-dependent fashion. The presence of 100 μg/ml of anti-rmMPO IgG in the culture medium increased ICAM-1, VCAM-1 and E-selectin transcripts in mGEC by 12.5, 7.5 and 10.5-fold, respectively. The control cells treated with normal rabbit IgG did not show any significant changes in the mRNAs of these adhesion molecules. Since ICAM-1, showed the highest increase in mRNA expression by anti-rmMPO IgG and, is a counter receptor for CD11b/CD18 integrins expressed abundantly in neutrophils, the following experiments were particularly focused on this molecule. The dose-dependent increase in ICAM-1 protein level in the anti-rmMPO IgG-treated mGEC was further confirmed by ELISA (Figure 2B). The mGEC treated

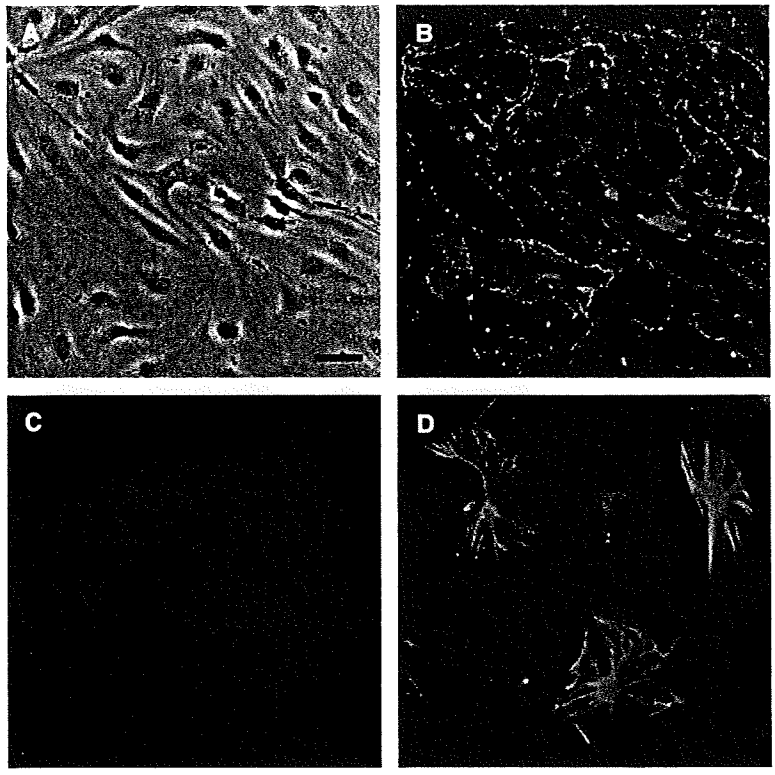

Fig. 1. Primary culture of mouse glomerular endothelial cells. Isolated mGEC were cultured on coverslips and phase contrast image (**A**) and immunofluorescence image for CD31 (**B**) were obtained in the same field. The mGEC were negatively stained by anti-desmin (**C**). Mesangial cells stained for desmin (**D**) served as a positive control. Bar = 20 μm.

with 100 μg/ml anti-rmMPO IgG for 6 h doubled the cellular ICAM-1 level and this condition was used for the following studies. In this condition, the increased expression of ICAM-1 by anti-rmMPO IgG was evident as shown by immunofluorescence microscopy for ICAM-1 (Figure 2C). In terms of cell morphology, there was no significant difference between anti-rmMPO IgG-treated cells and control normal IgG-treated cells (data not shown).

Involvement of rmMPO-specific antibodies in up-regulation of ICAM-1 expression in mGEC

To rule out the possibility of enhanced adhesion molecule expression by some contaminated substances, various concentrations of anti-rmMPO IgG were incubated with or without protein A sepharose beads for 1 h at 4°C and then the supernatants were used for assays. Anti-rmMPO activity was almost diminished at any concentration by incubation with protein A sepharose beads (Figure 3A). Similarly, the expression of ICAM-1 returned to control level by the depletion of IgG (Figure 3B), indicating that the enhancement of the ICAM-1 expression was induced only by the IgG molecules in anti-rmMPO IgG.

Since the polyclonal antibodies to rmMPO were used in this study, to rule out the up-regulation by non-specific IgGs, the experiment was conducted to confirm that the effects were induced by rmMPO-specific IgG. Recombinant mMPO-specific IgG was adsorbed by incubating with aggregated rmMPO protein, and titre of the resultant supernatant was determined by ELISA. Figure 4A shows the anti-rmMPO reactivity before and after incubation with aggregated rmMPO. The titre in adsorbed antibody decreased to approximately half of the non-adsorbed control. The degree of up-regulation of ICAM-1 expression was also decreased in the cells treated by the adsorbed antibody as compared with the original anti-rmMPO IgG (Figure 4B). Therefore, the increased expression of ICAM-1 seemed to be mediated by the rmMPO-specific IgG molecules and the molecular specificity of the antibody is one of the important factors in the activation.

To investigate the importance of molecular specificity, anti-rmMPO IgG was cleaved into $F(ab')_2$ and Fc fragments by incubating with pepsin (Figure 5A) and the $F(ab')_2$ portion was tested for its ability to up-regulate ICAM-1 expression. As shown in Figure 5B, since there was a significant decrease in the activity of the antibody even after the incubation in sodium acetate buffer without pepsin, the concentration of antibody tested was increased up to 1000 μg/ml. The loss of activity seemed to be due to low-pH-induced denaturation of IgG molecules in the process of digestion in sodium acetate buffer (pH 4.5). The $F(ab')_2$ portion of anti-rmMPO IgG induced a significant increase in ICAM-1 expression in a dose-dependent manner, although it had less activity than the antibody incubated in acetate buffer

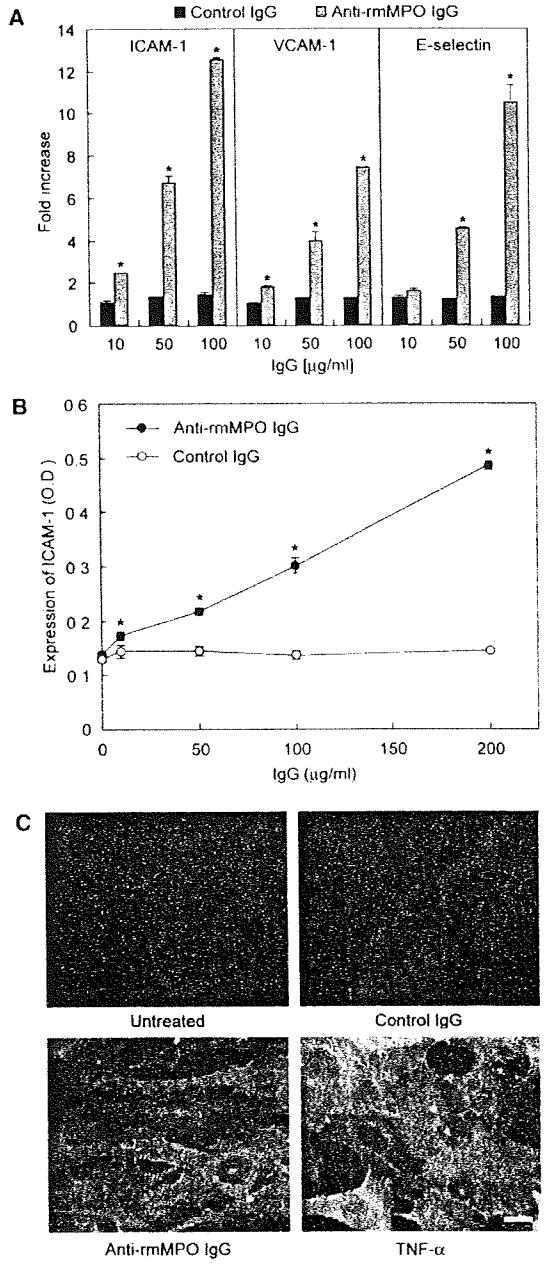

Fig. 2. Up-regulation of adhesion molecule expression in mGEC induced by anti-rmMPO IgG. (**A**) Total RNA was extracted from the mGEC treated with either anti-rmMPO IgG or control rabbit IgG for 4 h. These RNA samples were subjected to real-time RT-PCR analysis as described in Materials and methods. The mRNA levels were normalized by that of non-treated control cells and shown as fold increase. $^*P < 0.05$ *vs* control IgG at same concentration. (**B**) The mGEC were incubated for 6 h with either anti-rmMPO IgG or control rabbit IgG with increasing concentrations. The cells were fixed and ICAM-1 expression level was evaluated by cell ELISA. Data are expressed by optical density at 405 nm. $^*P < 0.05$ *vs* control IgG at same concentration. (**C**) The mGEC were treated with either 100 μg/ml anti-rmMPO or control IgG and then immunostained for ICAM-1 as described in Materials and methods. TNF-α-treated cells served as a positive control. Bar = 20 μm.

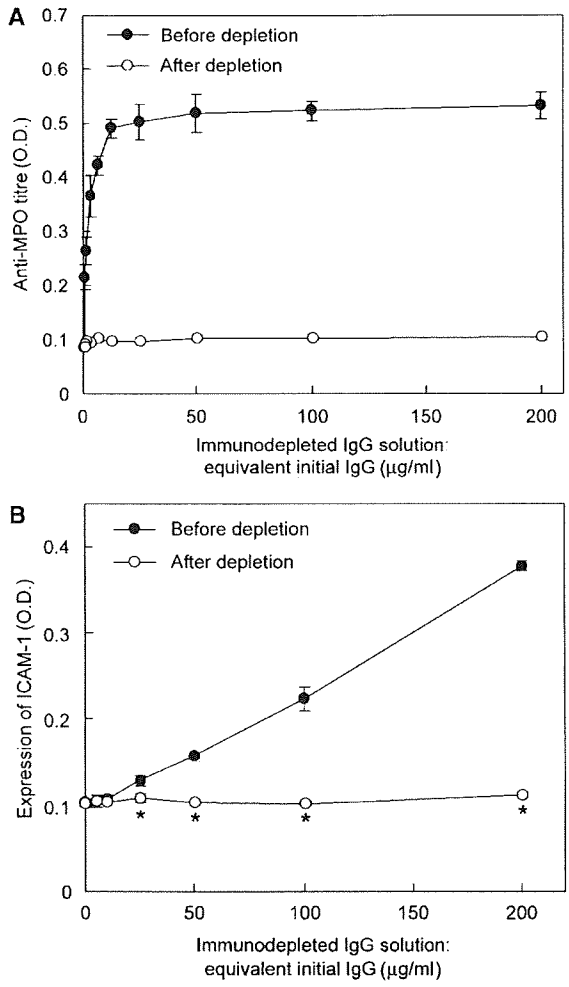

Fig. 3. Up-regulation of ICAM-1 is induced only by IgG molecules and is not attributable to contaminated substances. Anti-rmMPO IgG was incubated with or without protein A sepharose for 1 h at 4°C. After incubation, sepharose beads were spun down and the supernatants were used for the experiments. **(A)** Anti-rmMPO titre of the supernatants was evaluated by ELISA. The anti-rmMPO titre was expressed by optical density at 405 nm. **(B)** mGEC were incubated with the supernatants for 6 h and ICAM-1 expression levels of the mGEC were measured by cell ELISA. Data are expressed by optical density at 405 nm. $^*P < 0.05$ *vs* IgG before depletion at the same concentration.

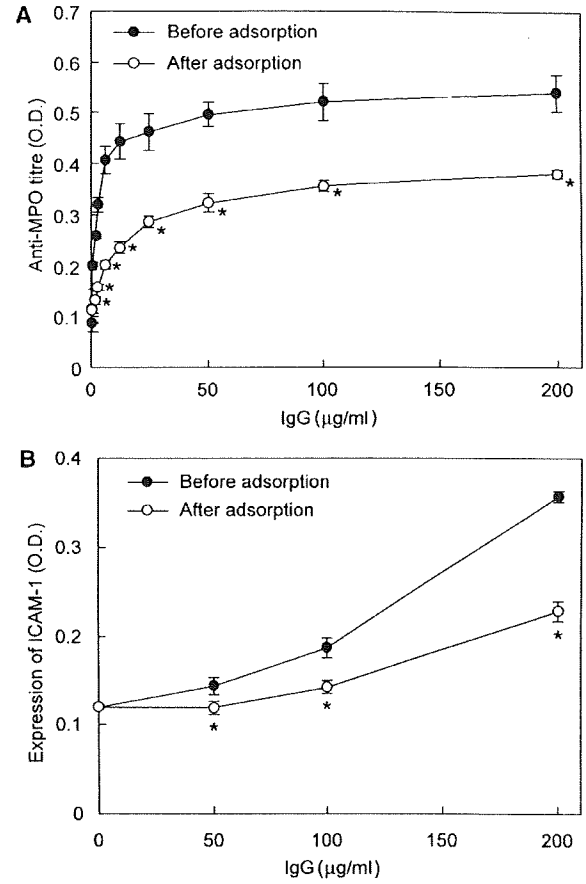

Fig. 4. Antibodies specific to rmMPO induce endothelial activation. MPO-specific IgG was adsorbed by incubating with aggregated rmMPO protein by batch method-like procedure as described in Materials and methods. Protein concentration of the adsorbed IgG was measured and then the IgG was used to measure antibody titre **(A)** and inducibility of ICAM-1 up-regulation **(B)**. Both anti-rmMPO titres and ICAM-1 expression levels are expressed by optical density at 405 nm. $^*P < 0.05$ *vs* IgG before adsorption at the same concentration.

without pepsin. The results demonstrate that the antigen specificity of the $F(ab')_2$ portion of anti-rmMPO IgG mediates the enhanced ICAM-1 expression in mGEC.

It has been reported that anti-endothelial cell antibodies from scleroderma or Behçet's disease patients induced adhesion molecule expression [20,21]. To check whether anti-endothelial activity of the anti-rmMPO IgG mediates the activation of the mGEC, anti-endothelial cell activity of anti-rmMPO IgG was compared with control normal rabbit IgG. As shown in Figure 6A, both anti-rmMPO and control IgG showed slight dose-dependent increases in binding to mGEC, which seemed to result mostly from non-specific binding of the antibodies. Contrary to ICAM-1 expression, the difference in the binding activity between control and anti-rmMPO antibodies was undetectable by ELISA. To examine whether antibody binding is specific for living cells, mGEC were treated with anti-rmMPO IgG for 4 h before fixation and bound anti-rmMPO IgG was quantified. As a result, the live mGEC showed binding kinetics similar to fixed mGEC (data not shown). Considering that antigen specificity of anti-rmMPO IgG was necessary to induce the enhanced ICAM-1 expression, a target molecule must be present in mGEC. To test whether there is a target antigen for anti-rmMPO IgG in mGEC, an immunoprecipitation study was performed with anti-rmMPO and control IgGs. As shown in Figure 6B, there were several bands on SYPRO Ruby stain of endothelial proteins specifically

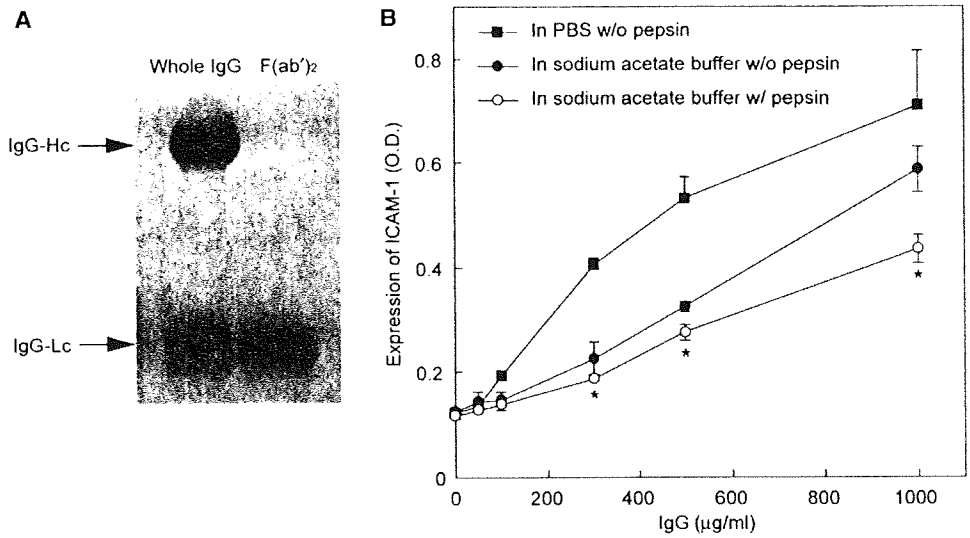

Fig. 5. Up-regulation of ICAM-1 expression in mGEC is associated with antigen specificity of $F(ab')_2$ portion of anti-rmMPO IgG. Anti-rmMPO IgG was digested into Fc and $F(ab')_2$ portions by incubating with pepsin in sodium acetate buffer. (**A**) The original IgG and the isolated $F(ab')_2$ were subjected to SDS-PAGE and stained with Coomassie Blue. (**B**) The $F(ab')_2$ fragments of anti-rmMPO were tested for the inducibility of enhanced ICAM-1 expression. For positive control, antibodies prepared by the same procedure except for incubation without pepsin were included in this experiment. Original anti-rmMPO incubated in PBS without pepsin was also prepared to check the effect of sodium acetate buffer. The ICAM-1 expression levels are expressed by optical density at 405 nm. $^*P < 0.05$ *vs* IgG incubated in sodium acetate buffer without pepsin at the same concentration.

immunoprecipitated with anti-rmMPO IgG. The molecular weights of these proteins did not correspond to those of precursor (90 kDa), heavy chain (57.5 kDa) or light chain (14 kDa) of MPO.

Up-regulation of TNF-α expression by anti-rmMPO IgG and its relation to adhesion molecule expression

In activated endothelial cells, a wide variety of cytokine genes are expressed other than adhesion molecules [27,28]. Inflammatory cytokines are the most important molecules expressed and secreted from the activated endothelial cells. Especially TNF-α is one such cytokine which contributes to the development of glomerulonephritis [13,24,29]. To examine whether the expression of TNF-α is involved in the activation of mGEC by anti-rmMPO IgG, TNF-α mRNA was measured by semi-quantitative RT–PCR. As shown in Figure 7A, the cells incubated for 6 h with various concentrations of anti-rmMPO IgG exhibited an increase in mRNA expression of TNF-α in a dose-dependent manner, whereas the control rabbit IgG failed to do so. Since TNF-α is one of the most potent endothelial activators and induces expression of adhesion molecules including ICAM-1, we examined the effect of neutralizing anti-TNF-α antibody on the enhanced expression of ICAM-1 in mGEC. The mGEC were treated with 100 μg/ml anti-rmMPO IgG in the presence of 0–20 μg/ml neutralizing anti-TNF-α antibody and the expression of ICAM-1 was evaluated. As shown in Figure 7B, there was no inhibition of the enhanced expression of ICAM-1 after 6 h. However, the endothelial activation was partially suppressed by neutralizing anti-TNF-α antibody in a dose-dependent manner if the cells were treated for 18 h.

Discussion

We have demonstrated that anti-rmMPO IgG induced an up-regulation of adhesion molecules. Johnson *et al.* [17] reported an enhanced expression of ICAM-1 in HUVEC with sera or purified IgG from patients with autoimmune vasculitis. However, the relationship between antigen recognition of the antibodies and the up-regulation of ICAM-1 has not been clear. In the present study, activating effects of 'MPO-specific' antibody on endothelial cells have been demonstrated. Since the $F(ab')_2$ fragment of anti-rmMPO IgG could also up-regulate the adhesion molecule, it was concluded that antigen recognition was involved in this process. However, we were unable to demonstrate whether cross-linking of the target antigen was involved because digestion and purification of Fab fragment led to loss of activity.

It has been reported earlier that MPO is not expressed in HUVEC [30] and we also confirmed by RT–PCR analysis that the isolated mGEC also do not express murine MPO (data not shown). The difference

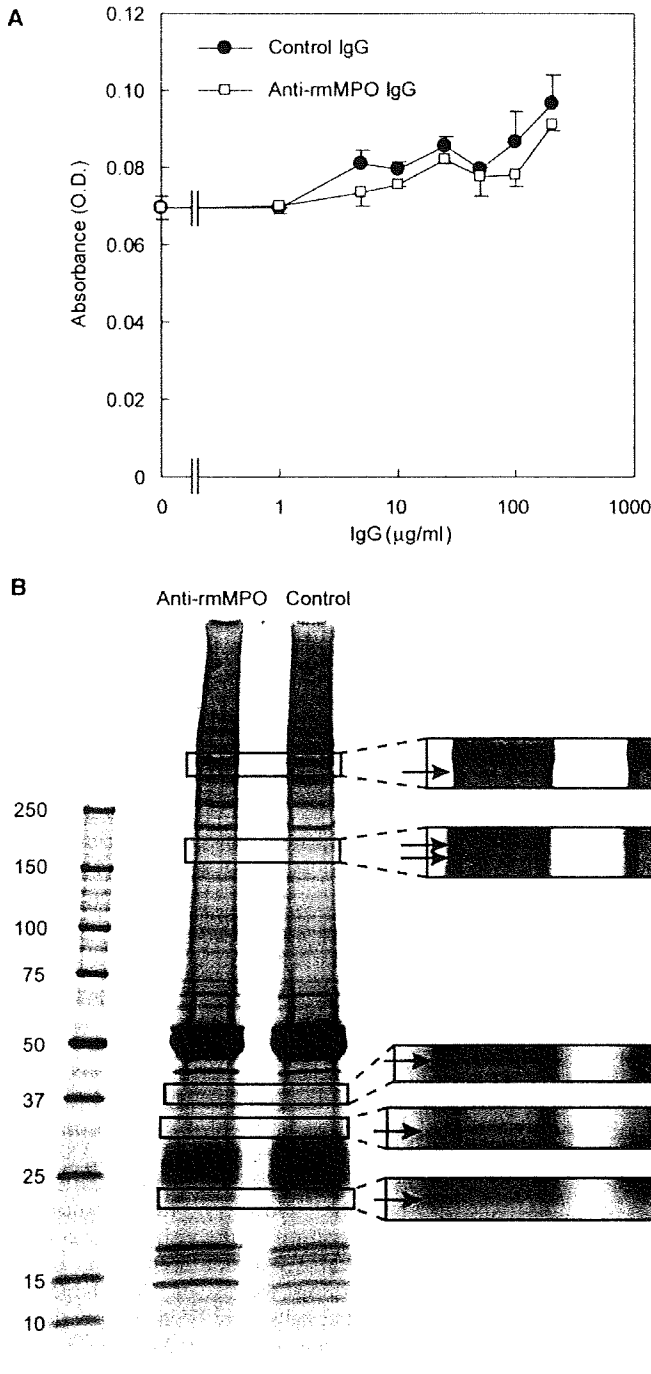

Fig. 6. Anti-endothelial activity of anti-rmMPO IgG. (**A**) Binding of anti-rmMPO IgG to fixed mGEC was evaluated by cell ELISA as described in Materials and methods. The anti-endothelial activities are expressed by optical density at 405 nm. (**B**) Immunoprecipitates from whole-cell lysate of mGEC either with anti-rmMPO or with control IgG were analysed by SDS-PAGE and SYPRO Ruby staining. The anti-rmMPO IgG-specific bands are magnified.

in anti-endothelial activity between anti-rmMPO and control rabbit IgG was undetectable by ELISA, presumably because non-specific binding (e.g. binding to Fc receptors) was dominant. However, since we successfully detected several bands on SYPRO Ruby stain of immunoprecipitates specific for anti-rmMPO IgG, we believe that only subtle binding of anti-rmMPO IgG to a certain molecule existing

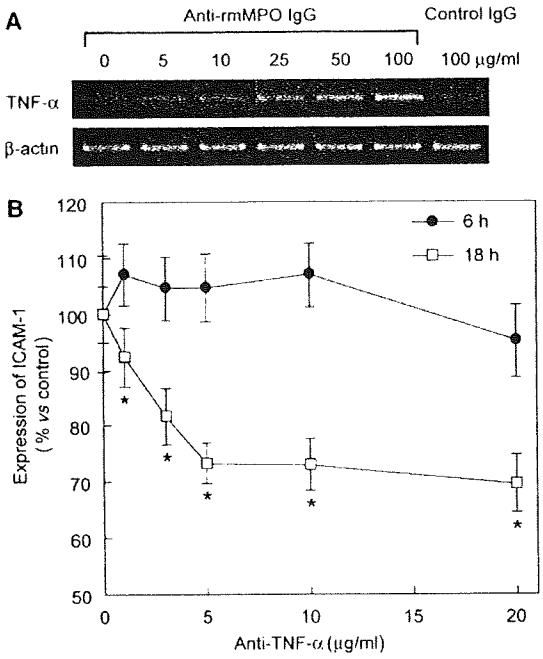

Fig. 7. Involvement of TNF-α expression in up-regulation of ICAM-1. (A) The mGEC were incubated with indicated concentrations of anti-rmMPO IgG or control rabbit IgG for 6 h and then mRNA expression of TNF-α was determined by semi-quantitative RT–PCR method. RT–PCR products of β-actin of the same samples were included as internal control. (B) Inhibition of up-regulation of ICAM-1 expression by neutralizing anti-TNF-α antibody. The mGEC were incubated for 6 or 18 h with 100 μg/ml anti-rmMPO IgG in the presence of the indicated concentrations of neutralizing anti-TNF-α antibodies. ICAM-1 expression levels of the cells were measured by cell ELISA and were normalized by that of the cells treated with 100 μg/ml anti-rmMPO IgG in the absence of neutralizing antibody. $^*P < 0.05$ *vs* cells treated with anti-rmMPO IgG in the absence of neutralizing antibody.

on mGEC can trigger the activation of mGEC. Therefore, we speculate that certain molecules expressed in mGEC (probably on plasma membrane) may share the epitope of anti-rmMPO IgG and transduce signals leading to the enhanced expressions of adhesion molecules. Identification of the molecules bound with anti-rmMPO IgG will be analysed in a future study.

Although it has been reported earlier that monoclonal antibodies against MPO do not induce endothelial activation [17], yet the present study shows its induction of adhesion molecules. We, however, here utilized the polyclonal anti-rmMPO IgG containing antibodies with many different binding sites (epitopes) to MPO. The reports, on epitope mapping of MPO-ANCA using recombinant deletion mutants of MPO, have demonstrated that MPO-ANCA in sera of the patients recognizes different epitope sites of MPO with a restricted number of epitopes located on heavy chain of MPO [31–33]. Furthermore, the epitope recognition profiles are also related to clinical features. In other words, only a few clones targeting the risk epitopes can initiate and progress MPO-ANCA-associated glomerulonephritis. Therefore, the polyclonal antibody used in this study seems to contain the antibodies against the specific risk epitopes. An epitope mapping of the anti-rmMPO IgG which activated mGEC in the present study may help to elucidate the cross-reactivity of anti-rmMPO IgG and the mechanism of endothelial activation related to pathogenicity of MPO-ANCA.

The results of the neutralizing anti-TNF-α antibody experiment show that although TNF-α was not likely to be a primary activator in the initial period (6 h), endothelial ICAM-1 expression was enhanced by TNF-α secreted from activated mGEC after 18 h. The production of TNF-α induced by anti-rmMPO IgG may in part contribute to the up-regulation of adhesion molecules in an autocrine fashion. However, it still remains controversial whether anti-rmMPO IgG directly induces the up-regulation of adhesion molecules because the other inflammatory mediators might be released from mGEC, and subsequently activate mGEC even just after the binding of anti-rmMPO IgG. Besides TNF-α, a wide variety of inflammatory cytokines or chemokines such as interleukin (IL)-1, IL-8 and monocyte chemoattractant protein-1 (MCP-1) are released from endothelial cells in response to stimuli [34,35]. These cytokines/chemokines activate endothelial cells and up-regulate ICAM-1 expression [36–38] and have been further reported to correlate with clinical presentation of MPO-ANCA-associated glomerulonephritis. Adhesion molecules, investigated in this study as well as TNF-α are mainly expressed through NF-κB activation [39–42]. Therefore, it is expected that anti-rmMPO IgG activated NF-κB which subsequently induced up-regulation of adhesion molecules and inflammatory cytokines/chemokines. Blocking antibodies to these cytokines/chemokines or inhibitor of NF-κB may further reveal the role of these mediators in up-regulation of adhesion molecules.

Sensitivity of endothelial cells to cytokine exposure or injury mediated by activated neutrophils differs with their origin [22,43]. We also examined the change in ICAM-1 expression by anti-rmMPO IgG using other microvascular endothelial cells such as primary mouse lung endothelial cells (mLEC) and pancreatic islet endothelial cell line (MS1). These cells also showed an increased mRNA expression of ICAM-1 (see 'Supplementary' data), indicating that these effects were commonly seen in microvascular endothelium and not limited in the kidney. MPO-ANCA is believed to be associated with the development of small vessel vasculitis. Therefore, the comparison of adhesion molecule expression by anti-rmMPO IgG between endothelial cells from small and large vessels might help to understand the pathogenesis of ANCA-associated vasculitis.

In conclusion, the present results clearly indicate that the anti-MPO antibody up-regulates the expression of ICAM-1, VCAM-1 and E-selectin in mGEC,

suggesting that not only neutrophils but also glomerular endothelial cells are activated by MPO-ANCA and contribute to neutrophil adhesion to GEC, thereby increasing glomerular neutrophil infiltration in initiation and progression of pauci-immune glomerulonephritis. It is still unknown how anti-rmMPO IgG stimulates the expression of adhesion molecules in mGEC, although our study revealed that antigen recognition of anti-rmMPO IgG is necessary for the stimulation. Future *in vitro* studies on the aforementioned issues will provide a more precise mechanism for endothelial activation in pauci-immune glomerulonephritis. Furthermore, using the animal model of MPO-ANCA-associated glomerulonephritis [44], we will investigate the role of MPO-ANCA-induced expression of adhesion molecules and inflammatory cytokines/chemokines in mGEC *in vivo*.

Acknowledgements. This study was in part supported by grants from Japan Human Science Foundation and Ministry of Health, Labour and Welfare, Japan.

Conflict of interest statement. None declared.

References

1. Falk RJ, Jennette JC. Anti-neutrophil cytoplasmic autoantibodies with specificity for myeloperoxidase and proteinase 3 in patients with systemic vasculitis and necrotizing crescentic glomerulonephritis. *N Engl J Med* 1988; 318: 1651–1657
2. Gross WL, Schmitt WH, Csernok E. ANCA and associated diseases: immunodiagnostic and pathogenetic aspects. *Clin Exp Immunol* 1993; 91: 1–12
3. Kallenberg CG, Brouwer E, Weening JJ, Tervaert JW. Antineutrophil cytoplasmic antibodies: current diagnostic and pathophysiological potential. *Kidney Int* 1994; 46: 1–15
4. De Oliviera J, Gaskin G, Dash A, Rees AJ, Pusey CD. Relationship between disease activity and anti-neutrophil cytoplasmic antibody concentration in long-term management of systemic vasculitis. *Am J Kidney Dis* 1995; 25: 380–389
5. Goeken JA. Antineutrophil cytoplasmic antibody—A useful serological marker for vasculitis. *J Clin Immunol* 1991; 11: 61–74
6. Ara J, Mirapeix E, Rodriguez R, Saurina A, Darnell A. Relationship between ANCA and disease activity in small vessel vasculitis patients with anti-MPO ANCA. *Nephrol Dial Transplant* 1999; 14: 1667–1672
7. Falk RJ, Terrell RS, Charles LA, Jannette JC. Anti-neutrophil cytoplasmic autoantibodies induce neutrophils to degranulate and produce oxygen radicals *in vitro*. *Proc Natl Acad Sci USA* 1990; 87: 4115–4119
8. Charles LA, Caldas ML, Falk RJ, Terrell RS, Jennette JC. Antibodies against granule proteins activate neutrophils *in vitro*. *J Leukoc Biol* 1991; 50: 539–546
9. Reumaux D, Vossebeld PJ, Roos D, Verhoeven AJ. Effect of tumor necrosis factor-induced integrin activation on Fc gamma receptor II-mediated signal transduction: relevance for activation of neutrophils by anti-proteinase 3 or anti-myeloperoxidase antibodies. *Blood* 1995; 86: 3189–3195
10. Kettritz R, Schreiber A, Luft FC, Haller H. Role of mitogen-activated protein kinases in activation of human neutrophils by antineutrophil cytoplasmic antibodies. *J Am Soc Nephrol* 2001; 12: 37–46
11. Kettritz R, Choi M, Butt W *et al.* Phosphatidylinositol 3-kinase controls antineutrophil cytoplasmic antibodies-induced respiratory burst in human neutrophils. *J Am Soc Nephrol* 2002; 13: 1740–1749
12. Rarok AA, Limburg PC, Kallenberg CG. Neutrophil-activating potential of antineutrophil cytoplasm autoantibodies. *J Leukoc Biol* 2003; 74: 3–15
13. Tesar V, Masek Z, Rychlik I *et al.* Cytokines and adhesion molecules in renal vasculitis and lupus nephritis. *Nephrol Dial Transplant* 1998; 13: 1662–1667
14. Ara J, Mirapeix E, Arrizabalaga P *et al.* Circulating soluble adhesion molecules in ANCA-associated vasculitis. *Nephrol Dial Transplant* 2001; 16: 276–285
15. Di Lorenzo G, Pacor ML, Mansueto P *et al.* Circulating levels of soluble adhesion molecules in patients with ANCA-associated vasculitis. *J Nephrol* 2004; 17: 800–807
16. Raab M, Daxecker H, Markovic S, Karimi A, Griesmacher A, Mueller MM. Variation of adhesion molecule expression on human umbilical vein endothelial cells upon multiple cytokine application. *Clin Chim Acta* 2002; 321: 11–16
17. Johnson PA, Alexander HD, McMillan SA, Maxwell AP. Up-regulation of the endothelial cell adhesion molecule intercellular adhesion molecule-1 (ICAM-1) by autoantibodies in autoimmune vasculitis. *Clin Exp Immunol* 1997; 108: 234–242
18. De Bandt M, Meyer O, Hakim J, Pasquier C. Antibodies to proteinase-3 mediate expression of intercellular adhesion molecule-1 (ICAM-1, CD 54). *Br J Rheumatol* 1997; 36: 839–846
19. Mayet WJ, Schwarting A, Orth T, Duchmann R, Meyer zum Buschenfelde KH. Antibodies to proteinase 3 mediate expression of vascular cell adhesion molecule-1 (VCAM-1). *Clin Exp Immunol* 1996; 103: 259–267
20. Carvalho D, Savage CO, Black CM, Pearson JD. IgG antiendothelial cell autoantibodies from scleroderma patients induce leukocyte adhesion to human vascular endothelial cells *in vitro*. Induction of adhesion molecule expression and involvement of endothelium-derived cytokines. *J Clin Invest* 1996; 97: 111–119
21. Triolo G, Accardo-Palumbo A, Triolo G, Carbone MC, Ferrante A, Giardina E. Enhancement of endothelial cell E-selectin expression by sera from patients with active Behçet's disease: moderate correlation with anti-endothelial cell antibodies and serum myeloperoxidase levels. *Clin Immunol* 1999; 91: 330–337
22. Murakami S, Morioka T, Nakagawa Y, Suzuki Y, Arakawa M, Oite T. Expression of adhesion molecules by cultured human glomerular endothelial cells in response to cytokines: comparison to human umbilical vein and dermal microvascular endothelial cells. *Microvasc Res* 2001; 62: 383–391
23. Deocharan B, Qing X, Lichauco J, Putterman C. α-actinin is a cross-reactive renal target for pathogenic anti-DNA antibodies. *J Immunol* 2002; 168: 3072–3078
24. Ishida-Okawara A, Ito-Ihara T, Muso E *et al.* Neutrophil contribution to the crescentic glomerulonephritis in SCG/Kj mice. *Nephrol Dial Transplant* 2004; 19: 1708–1715
25. Johnson N, Mansfield KL, Fooks AR. Canine vaccine recipients recognize an immunodominant region of the rabies virus glycoprotein. *J Gen Virol* 2002; 83: 2663–2669
26. Livak KJ, Schmittgen TD. Analysis of relative gene expression data using real-time quantitative PCR and the $2^{-\Delta\Delta CT}$ method. *Methods* 2001; 25: 402–408
27. Mayer H, Bilban M, Kurtev V *et al.* Deciphering regulatory patterns of inflammatory gene expression from interleukin-1-stimulated human endothelial cells. *Arterioscler Thromb Vasc Biol* 2004; 24: 1192–1198
28. Franscini N, Bachli EB, Blau N, Leikauf MS, Schaffner A, Schoedon G. Gene expression profiling of inflamed human endothelial cells and influence of activated protein C. *Circulation* 2004; 110: 2903–2909
29. Arimura Y, Minoshima S, Kamiya Y *et al.* Serum myeloperoxidase and serum cytokines in anti-myeloperoxidase antibody-associated glomerulonephritis. *Clin Nephrol* 1993; 40: 256–264

30. Pendergraft WF, Alcorta DA, Segelmark M *et al.* ANCA antigens, proteinase 3 and myeloperoxidase, are not expressed in endothelial cells. *Kidney Int* 2000; 57: 1981–1990
31. Tomizawa K, Mine E, Fujii A *et al.* A panel set for epitope analysis of myeloperoxidase (MPO)-specific antineutrophil cytoplasmic antibody MPO-ANCA using recombinant hexamer histidine-tagged MPO deletion mutants. *J Clin Immunol* 1998; 18: 142–152
32. Fujii A, Tomizawa K, Arimura Y *et al.* Epitope analysis of myeloperoxidase (MPO) specific anti-neutrophil cytoplasmic autoantibodies (ANCA) in MPO-ANCA-associated glomerulonephritis. *Clin Nephrol* 2000; 53: 242–252
33. van der Geld YM, Stegeman CA, Kallenberg CG. B cell epitope specificity in ANCA-associated vasculitis: does it matter? *Clin Exp Immunol* 2004; 137: 451–459
34. Libby P, Ordovas JM, Auger KR, Robbins AH, Birinyi LK, Dinarello CA. Endotoxin and tumor necrosis factor induce interleukin-1 gene expression in adult human vascular endothelial cells. *Am J Pathol* 1986; 124: 179–185
35. Brown Z, Gerritsen ME, Carley WW, Strieter RM, Kunkel SL, Westwick J. Chemokine gene expression and secretion by cytokine-activated human microvascular endothelial cells. Differential regulation of monocyte chemoattractant protein-1 and interleukin-8 in response to interferon-γ. *Am J Pathol* 1994; 145: 913–921
36. Bochner BS, Luscinskas FW, Gimbrone MA,Jr *et al.* Adhesion of human basophils, eosinophils and neutrophils to interleukin 1-activated human vascular endothelial cells: contributions of endothelial cell adhesion molecules. *J Exp Med* 1991; 173: 1553–1557
37. Haraldsen G, Kvale D, Lien B, Farstad IN, Brandtzaeg P. Cytokine-regulated expression of E-selectin, intercellular adhesion molecule-1 (ICAM-1) and vascular cell adhesion molecule-1 (VCAM-1) in human microvascular endothelial cells. *J Immunol* 1996; 156: 2558–2565
38. Raab M, Daxecker H, Markovic S, Karimi A, Griesmacher A, Mueller MM. Variation of adhesion molecule expression on human umbilical vein endothelial cells upon multiple cytokine application. *Clin Chim Acta* 2002; 321: 11–16
39. Ledebur HC, Parks TP. Transcriptional regulation of the intercellular adhesion molecule-1 gene by inflammatory cytokines in human endothelial cells. Essential roles of a variant NF-κB site and p65 homodimers. *J Biol Chem* 1995; 270: 933–943
40. Shu HB, Agranoff AB, Nabel EG *et al.* Differential regulation of vascular cell adhesion molecule 1 gene expression by specific NF-κB subunits in endothelial and epithelial cells. *Mol Cell Biol* 1993; 13: 6283–6289
41. Whelan J, Ghersa P, Hooft van Huijsduijnen R *et al.* An NFκB-like factor is essential but not sufficient for cytokine induction of endothelial leukocyte adhesion molecule 1 (ELAM-1) gene transcription. *Nucleic Acids Res* 1991; 19: 2645–2653
42. Chan EL, Haudek SB, Giroir BP, Murphy JT. Human coronary endothelial cell activation by endotoxin is characterized by NF-κB activation and TNF-α synthesis. *Shock* 2001; 16: 349–354
43. Murphy HS, Bakopoulos N, Dame MK, Varani J, Ward PA. Heterogeneity of vascular endothelial cells: differences in susceptibility to neutrophil-mediated injury. *Microvasc Res* 1998; 56: 203–211
44. Xiao H, Heeringa P, Hu P *et al.* Antineutrophil cytoplasmic autoantibodies specific for myeloperoxidase cause glomerulonephritis and vasculitis in mice. *J Clin Invest* 2002; 110: 955–963

Received for publication: 14.4.06
Accepted in revised form: 18.8.06